

Simulation of crowd evacuation under attack considering emotion spreading

Yang Wang(王杨), Ning Ding(丁宁), Dapeng Dong(董大鹏), and Yu Zhu(朱萸)
Citation: Chin. Phys. B, 2024, 33 (**12**): 128901. DOI: 10.1088/1674-1056/ad84c7
Journal homepage: http://cpb.iphy.ac.cn; http://iopscience.iop.org/cpb

What follows is a list of articles you may be interested in

An extended social force model on unidirectional flow considering psychological and behavioral impacts of hazard source

Kaifeng Deng(邓凯丰), Meng Li(李梦), Xiangmin Hu(胡祥敏), and Tao Chen(陈涛)
Chin. Phys. B, 2024, 33 (**2**): 028901. DOI: 10.1088/1674-1056/ad1173

Passenger management strategy and evacuation in subway station under Covid-19

Xiao-Xia Yang(杨晓霞), Hai-Long Jiang(蒋海龙), Yuan-Lei Kang(康元磊), Yi Yang(杨毅), Yong-Xing Li(李永行), and Chang Yu(蔚畅)
Chin. Phys. B, 2022, 31 (**7**): 078901. DOI: 10.1088/1674-1056/ac43b3

Spatial memory enhances the evacuation efficiency of virtual pedestrians under poor visibility condition

Yi Ma(马毅), Eric Wai Ming Lee(李伟民), Meng Shi(施朦), Richard Kwok Kit Yuen(袁国杰)
Chin. Phys. B, 2018, 27 (**3**): 038901. DOI: 10.1088/1674-1056/27/3/038901

Analysis of dynamic features in intersecting pedestrian flows

Hai-Rong Dong(董海荣), Qi Meng(孟琦), Xiu-Ming Yao(姚秀明), Xiao-Xia Yang(杨晓霞), Qian-Ling Wang(王千龄)
Chin. Phys. B, 2017, 26 (**9**): 098902. DOI: 10.1088/1674-1056/26/9/098902

Pedestrian evacuation at the subway station under fire

Xiao-Xia Yang(杨晓霞), Hai-Rong Dong(董海荣), Xiu-Ming Yao(姚秀明), Xu-Bin Sun(孙绪彬)
Chin. Phys. B, 2016, 25 (**4**): 048902. DOI: 10.1088/1674-1056/25/4/048902

Simulation of crowd evacuation under attack considering emotion spreading

Yang Wang(王杨)[1,2], Ning Ding(丁宁)[1,2,3,†], Dapeng Dong(董大鹏)[1], and Yu Zhu(朱萸)[4]

[1] *Public Security Behavioral Science Laboratory, People's Public Security University of China, Beijing* 100084, *China*
[2] *School of Public Order, People's Public Security University of China, Beijing* 100084, *China*
[3] *Center For Capital Social Safety, People's Public Security University of China, Beijing* 100084, *China*
[4] *Institute of Public Safety Research, Department of Engineering Physics, Tsinghua University, Beijing* 100084, *China*

(Received 15 July 2024; revised manuscript received 20 September 2024; accepted manuscript online 9 October 2024)

In recent years, attacks against crowded places such as campuses and theaters have had a frequent and negative impact on the security and stability of society. In such an event, the crowd will be subjected to high psychological stress and their emotions will rapidly spread to others. This paper establishes the attack–escape evacuation simulation model (AEES-SFM), based on the social force model, to consider emotion spreading under attack. In this model, (1) the attack–escape driving force is considered for the interaction between an attacker and evacuees and (2) emotion spreading among the evacuees is considered to modify the value of the psychological force. To validate the simulation, several experiments were carried out at a university in China. Comparing the simulation and experimental results, it is found that the simulation results are similar to the experimental results when considering emotion spreading. Therefore, the AEES-SFM is proved to be effective. By comparing the results of the evacuation simulation without emotion spreading, the emotion spreading model reduces the evacuation time and the number of casualties by about 30%, which is closer to the real experimental results. The results are still applicable in the case of a 40-person evacuation. This paper provides theoretical support and practical guidance for campus response to violent attacks.

Keywords: violent attacks, crowd evacuation, social force model, emotion spreading

PACS: 89.20.–a, 89.40.–a, 07.05.Tp **DOI:** 10.1088/1674-1056/ad84c7

1. Introduction

Terrorist attacks tend to be organized, premeditated violent crimes, often occurring in venues with a high degree of attention and a certain degree of political interest. Compared with terrorist attacks, extreme violent attacks due to social injustice or personal psychological reasons occur more frequently in society. Although smaller in scale, the randomness and unpredictability of individual events of extreme violence pose greater challenges to emergency management. For example, on 27 March 2023, an assailant killed six people at Covenant School in Nashville, Tennessee. While these types of violent crimes cause many deaths, they also leave horrible memories for others, especially students, which can lead to psychological problems such as anorexia and phobias.[1] Researchers have studied different aspects with the aim of preventing violent attacks and reducing casualties, but there are fewer studies on emergency evacuation.

The fact that most of the violent attackers on campuses are from outside the school and that the time, manner and cause of the attack are randomized has led to the fact that prevention policies aimed at students have had little effect on the prevention of violent attacks.[2] Violent attacks inevitably occur from time to time when prevention strategies are ineffective, and personal escape strategies play an important role in minimizing the number of casualties. Unlike the United States, China has stringent gun control laws. As a result, attackers now mostly utilize tools such as knives and axes to attack at universities.[3–5] Therefore, with campuses at risk of violent attacks, rapid and effective emergency evacuation is critical to student safety.[6] When evacuating during a fire or earthquake, staying away from fixed 'sources of danger' such as buildings is all that is required to constitute a successful evacuation. However, during a physical attack evacuees are choosing their evacuation routes based on the attacker's attack behavior to remain out of the attacker's range and reach a relatively safe location. Successful evacuation is defined as fleeing to a location unharmed by the attack. This leads to the potential failure of conventional evacuation plans based on fire-related scenes.[7]

Researchers have proposed many simulation models to study the impact of attackers on crowd evacuation behavior, with the social force model being used.[8] Social force modeling better describes the movement patterns of evacuating crowds and interactions between crowds.[9–11] Liu investigated the effects of assailants and egress on the number of casualties based on the social force model.[12] Arteaga and Jee combined the social force model with the intelligent body model to study the effect of building parameters on pedestrian evacuation efficiency during a shooting incident in a building, and found that the width of the hall and the width of the

†Corresponding author. E-mail: dingning_thu@126.com

© 2024 Chinese Physical Society and IOP Publishing Ltd

door had the greatest positive effect on the evacuees' escape behavior.[13] Liu *et al.* considered the impact of psychological elements on the evacuation behaviors of evacuees as well as interactions between the evacuees and their attackers by combining the social force model with the Yerkes–Dodson law.[14] Researchers have conducted some studies on the effects of the interaction between attackers and evacuees on evacuation during violent attacks through simulation modeling, but model accuracy could be further improved.

It is important to note that during an emergency evacuation, evacuees can easily become highly stressed due to the suddenness and danger of the event, thus preventing most people from making rational decisions.[15] However, the impact on different people in the same dangerous situation is not the same, which is reflected in the differences in the ability of different evacuees to receive information and their psychological tolerance.[16] In violent attacks, the evacuees quickly generate significant nervous emotion and spread it to one another, which has a higher effect on evacuation effectiveness.

In this paper, we consider the emotional spreading of the evacuees and add the 'attack–escape' driving force based on the social force model, simulating the 'dynamic interaction' between the evacuees and the attackers to establish the attack–evacuation evacuation simulation model (AEES-SFM). Two typical Chinese university classroom layouts are reproduced in the simulation, and the AEES-SFM is applied to simulate the evacuation behaviors of incoming attackers attacking the two classrooms through different attack paths. The effectiveness of the AEES-SFM is also verified by conducting attack evacuation experiments in classrooms that are consistent with the simulation scenarios.

2. Modeling

2.1. Social force model and previous modified models

The social force model proposed by Helbing brought a new development to simulation modeling,[17] as shown in the following equation:

$$m_i\frac{\mathrm{d}\boldsymbol{v}_i}{\mathrm{d}t} = m_i\frac{v_i^0(t)\,\boldsymbol{e}_i^0(t)-\boldsymbol{v}_i(t)}{\tau_i} + \sum_{j(\neq i)} f_{ij} + \sum_W f_{iW}, \tag{1}$$

where m_i is the mass of the individual, $\boldsymbol{v}_i$ denotes the velocity vector of the individual, $v_i^0(t)$ denotes the magnitude of the desired velocity of the individual, $\boldsymbol{e}_i^0(t)$ denotes the direction of the desired velocity of the individual, f_{ij} denotes the interaction between the individual i and the other individual j, which includes both contact and non-contact forces, and f_{iW} denotes the interaction between the individual and an obstacle such as a wall, which also consists of both contact and non-contact forces.

Since the interactions between personnel and personnel and between personnel and obstacles are very similar in the social force model, Eq. (1) is rewritten here by replacing the original categorization according to the source of the force with the categorization according to the nature of the force to obtain

$$m_i\frac{\mathrm{d}\boldsymbol{v}_i}{\mathrm{d}t} = \boldsymbol{F}_{Di} + \boldsymbol{F}_{Si} + \boldsymbol{F}_{Gi}, \tag{2}$$

where $\boldsymbol{F}_{Di}$ denotes the self-driving force of individual i, $\boldsymbol{F}_{Si}$ denotes the psychological force on individual i, t denotes time, m_i denotes the mass of person i, and $\boldsymbol{v}_i$ is the velocity of person i. The self-driving force $\boldsymbol{F}_{Di}$ is given by

$$\boldsymbol{F}_{Di} = m_i\frac{\boldsymbol{v}_i^0-\boldsymbol{v}_i(t)}{\tau}, \tag{3}$$

where $\boldsymbol{v}_i^0$ denotes the desired velocity of evacuee i, $\boldsymbol{v}_i(t)$ is the velocity of person i at moment t and τ is the characteristic time.

The psychological force $\boldsymbol{F}_{Si}$ is the vector sum of the psychological forces that evacuee i is subjected to by all other evacuees j as well as the obstacle w, as shown in Eq. (4), while the social force $\boldsymbol{F}_{Sij}$ generated by other evacuees j is shown in Eq. (5);

$$\boldsymbol{F}_{Si} = \sum\nolimits_j \boldsymbol{F}_{Sij} + \sum\nolimits_w \boldsymbol{F}_{Siw}, \tag{4}$$

$$\boldsymbol{F}_{Sij} = A\,\mathrm{e}^{\varepsilon_{ij}/B}\left[\lambda+(1-\lambda)\frac{1+\cos\theta_{ij}}{2}\right](-\boldsymbol{n}_{ij}). \tag{5}$$

Here A and B are constants that measure the strength and range of action of the psychological force, ε_{ij} denotes the distance between evacuees i and j,

$$\varepsilon_{ij} = d_{ij} - r_i - r_j, \tag{6}$$

where r_i and r_j are the radii of evacuees i and j, and d_{ij} is the distance between the centers of mass of i and j. The direction of $\boldsymbol{F}_{Sij}$ is denoted by $-\boldsymbol{n}_{ij}$, which is a unit vector pointing from evacuee j to evacuee i. The parameter λ characterizes the anisotropy of the social force. θ_{ij} denotes the angle between the vectors $\boldsymbol{v}_i$ and $\boldsymbol{n}_{ij}$. The psychological force $\boldsymbol{F}_{Siw}$ generated by the obstacle w can be obtained similarly.

The contact of evacuee i with other people or obstacles generates a physical force $\boldsymbol{F}_{Gi}$, where the physical force $\boldsymbol{F}_{Gi}$ is shown in Eq. (7). Where evacuee i is subjected to an obstacle such as a wall, w generates a physical force $\boldsymbol{F}_{Giw}$ as shown in Eq. (8);

$$\boldsymbol{F}_{Gi} = \sum\nolimits_j \boldsymbol{F}_{Gij} + \sum\nolimits_w \boldsymbol{F}_{Giw}, \tag{7}$$

$$\boldsymbol{F}_{Giw} = \kappa g(\varepsilon_{iw})\boldsymbol{n}_{iw} + \mu g(\varepsilon_{iw})(-\boldsymbol{v}_{iw}\cdot\boldsymbol{t}_{iw})\boldsymbol{t}_{iw}, \tag{8}$$

where κ and μ are normal quantities indicating the strength of the elastic force and friction force, respectively, $\boldsymbol{v}_{iw}$ denotes the velocity of evacuee i to obstacle w and $\boldsymbol{t}_{iw}$ denotes the tangential unit vector between evacuee i and obstacle w. Physical

forces are generated only when an evacuee is in physical contact with an obstacle, so the function $g(\varepsilon_{iw})$ is greater than ε_{iw} and 0. $\boldsymbol{F}_{Gij}$ is found identically.

Gao *et al.*[18] improved the social force model by dividing the psychological forces in the social force model into collision-avoidance force and time-headway force and proposed the expected collision time, as shown below:

$$\boldsymbol{F}_{Si} = \boldsymbol{F}_{Si}^{\mathrm{H}} + \boldsymbol{F}_{Si}^{\mathrm{C}}, \tag{9}$$

$$\boldsymbol{F}_{Si}^{\mathrm{H}} = \begin{cases} -m_i \dfrac{v_i^0}{\tau}, & T^{\mathrm{H}} < \tau, \\ 0, & T^{\mathrm{H}} \geq \tau, \end{cases} \tag{10}$$

$$\boldsymbol{F}_{Si}^{\mathrm{C}} = \begin{cases} -m_i \dfrac{v_{ij} \cdot n_{ij}}{\tau}, \\ 0, \ T^{\mathrm{C}} \geq \tau, \end{cases} \tag{11}$$

where

$$T^{\mathrm{H}} = \frac{\left|d_{ij} \cdot \cos\theta\right| - \sqrt{(2R)^2 - (d_{ij} \cdot \sin\theta)^2}}{|v_i|}, \tag{12}$$

$$T^{\mathrm{C}} = \frac{\left|d_{ij} \cdot \cos\varphi\right| - \sqrt{(2R)^2 - (d_{ij} \cdot \sin\varphi)^2}}{\left|v_{ij}\right|}. \tag{13}$$

Ding *et al.*[19] modified the determination condition of psychological force on this basis to eliminate the oscillation phenomenon in the social force model, as shown below:

$$\boldsymbol{T}^{\mathrm{C}} = \frac{-\boldsymbol{v}_{ji} + \sqrt{\boldsymbol{v}_{ji}^2 + 2\boldsymbol{a}_{ji}(\boldsymbol{d}_{ij}\cos\varphi - \sqrt{(2r)^2 - (\boldsymbol{d}_{ij}\sin\varphi)^2})}}{\boldsymbol{a}_{ji}}, \tag{14}$$

where $\cos\varphi$ and $\sin\varphi$ are given by

$$\cos\varphi = \frac{\boldsymbol{d}_{ji} \cdot \boldsymbol{v}_{ji}}{|\,\boldsymbol{d}_{ji}\,||\,\boldsymbol{v}_{ji}\,|}, \quad \sin\varphi = \frac{\boldsymbol{d}_{ji} \cdot \boldsymbol{v}_{ji}}{|\,\boldsymbol{d}_{ji}\,||\,\boldsymbol{v}_{ji}\,|}. \tag{15}$$

The collision-avoidance psychological force describes the collision avoidance distance between evacuees i and j with psychological factors. When evacuees face attacks the presence of the attacker will cause evacuees to panic too much and the need to maintain a proper safe distance from the attacker is more urgent; they are more inclined to maintain a proper safe distance from the attacker to avoid violent attacks and then choose the right time to escape. Therefore, in this paper, the interactions between attackers and evacuees are captured by improving the collision-avoidance psychological force and adding the attack–escape driving force to the social force model.

2.2. Model of emotion spreading

The presence of attackers complicates crowd evacuation behavior. Interviews with participants have shown that people tend to be influenced by the emotions of others when facing a violent attack, leading to further panic and confusion.[20] Therefore, this paper establishes a model for the spread of evacuees' nervousness so that the simulation is more in line with their actual behavior.

When the nervous emotion of pedestrian evacuation is higher, the degree of tolerance for crowding and collision is also higher, and the requirement for personal space is also reduced. Under the support of this theory, the psychological force in the social force model is modified to obtain

$$\boldsymbol{F}_S^q = (1 - q(t))\,\boldsymbol{F}_S, \tag{16}$$

where the parameter $q_i(t)$ indicates the nervous emotion during evacuation of individual i at the moment t. Within the value range of (0,1), when $q = 0$ the individual will move according to the full value of the psychological force, and when $q = 1$ the individual will not be affected by the psychological force. Since the psychological force has the effect of counteracting the self-driving force to slow down the acceleration, the larger the value of q is the more tolerant the pedestrian is to the collision behavior. The model references the spiral transmission model proposed by Bosse *et al.*[21,22] in 2009 for a discussion of the transmission of nervous emotion between pedestrians during evacuation.

In an interactive process, each pedestrian has the identity of both the sender and the receiver of the psychological state, which forms the basic framework for the mutual dissemination of psychological factors in the evacuation process. As shown in Fig. 1(a), the information related to the sender of the nervous emotion is labeled with the subscript S, and the information related to the receiver is labeled with the subscript R. As shown in Fig. 1(b) for the interaction process between a single nervous emotion sender and a single receiver in an evacuation, under each moment t each person has the current evacuation nervous emotion measures q_S and q_R. For the propagators of psychological state, according to individuals' different personality traits and behavioral preferences, who possess different expression tendencies, those who are more inclined to express their internal states have a greater influence on the surrounding pedestrians. The degree of an individual's preference for expression is represented by the parameter $\varepsilon_S \in (0, 1)$. For the receiver of the psychological state, according to each person's personality traits, the ability to recognize the psychological state conveyed by the surrounding pedestrians is different. For example, pedestrians who are sensitive and observant at heart can obtain more information from the gestures, voices, facial expressions and other factors of the surrounding pedestrians, and are more able to experience the changes in the nervous emotions of the surrounding pedestrians during evacuation, while some pedestrians can only feel the current changes in urgency for evacuation through the pushing and shoving and acceleration of pedestrians. The receiver's sensitivity to the

psychological states of others is represented by the parameter $\delta_R \in (0, 1)$. Both psychological expression preference ε_S and degree of psychological sensitivity δ_R are closely related to an individual's personality traits, which will be more different between people but less related to the environment. To complete the process of transmitting the psychological state of nervous emotion from the sender to the receiver during evacuation, it is also necessary to consider the channel strength of the psychological state spread α. Intuitively, with the increase in distance between pedestrians, the effect of the sender is bound to decay. Therefore, in this paper, the channel strength of the spread of the psychological state between pedestrians is simply defined as the inverse of the distance

$$\alpha_{SR} = \frac{1}{|d_{SR}|}. \tag{17}$$

Based on the above analysis, we define the intensity of the influence of the psychological state γ_{SR} between individuals as in Eq. (18). If $\gamma_{SR} = 0$, it means that the current group of individuals shows no interactions of psychological states at all. If $\gamma_{SR} = 1$, the current receiver is maximally influenced by the propagator of that psychological state. It is evident that when γ_{SR} is not 0, the receivers can all feel each other's nervous emotion during evacuation from the sender, and the higher the value of γ_{SR}, the more influenced they are. Then at this time, the change in the situation of the receiver's nervous emotion during evacuation can be described by Eq. (19), where $\hat{q}$ denotes the degree of urgency that the receiver expects to achieve under the influence of others

$$\gamma_{SR} = \varepsilon_S \alpha_{SR} \delta_R, \tag{18}$$

$$\left.\frac{\mathrm{d}q(t)}{\mathrm{d}t}\right|_S = \varepsilon_S \alpha_{SR} \delta_R (\hat{q} - q(t)) = \gamma_{SR}(\hat{q} - q(t)). \tag{19}$$

The degree of urgency of the evacuation behavior is only an artificial definition of the psychological state, and a value between 0 and 1 is only symbolic and cannot be used as a real quantitative evaluation index. Consequently, it is not sufficient to categorize pedestrians' psychological states as high or low; rather, the effect on the recipient should be considered simultaneously from the perspectives of 'emergency' and 'non-emergency'. Different individuals have different receptive preferences for different types of psychological states, for example some pedestrians are more likely to be affected by the agitation and excitement of the pedestrians around them and become impatient, while others are more likely to feel the calmness of the people around them and become more relaxed. Therefore, the effect of the influence of the communicator's psychological state is categorized here in terms of positive and negative, which are denoted by $\hat{q}_{\mathrm{U}}$ and $\hat{q}_{\mathrm{D}}$, respectively. Figure 1(b) briefly illustrates the effect of the nervous evacuation emotion of the sender of the psychological state on the receiver in different trend directions, where equal proportionality logic was chosen for calculating the change values.

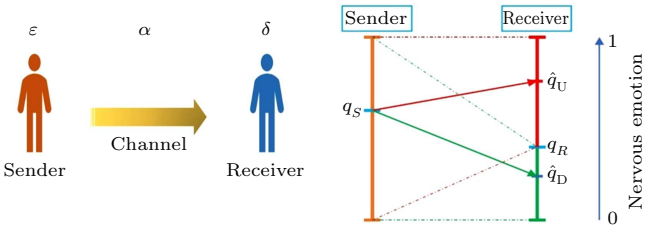


Fig. 1. Nervous emotion spreading of pedestrians: (a) emotion spreading between pedestrians and (b) changes in nervous emotion during evacuation.

Considering the direction of the 'urgency' trend, in the range of (0,1), the communicator's psychological state increases from 0 to q_S. For the receiver of the psychological state, the existing state is $1 - q_R$, then according to the logic of equal proportionality, the upsurge value in the current receiver's nervousness is $q_S(1 - q_R)$, so the result for upsurge of nervousness during evacuation can be obtained as shown in Eq. (20). Similarly, considering the 'non-urgent' trend, the propagator's psychological state changes from 1 to q_S; at this time, the psychological state of the receiver of the existing decline in the space of q_R, in the logic of equal proportionality of the receiver of the decline in nervousness, is $(1 - q_S)q_R$, so that the decline in nervousness during the evacuation can be obtained as shown in Eq. (21)

$$\hat{q}_{\mathrm{U}} = q_R + q_S(1 - q_R) = 1 - (1 - q_S)(1 - q_R), \tag{20}$$

$$\hat{q}_{\mathrm{D}} = q_R - (1 - q_S) q_R = q_S q_R. \tag{21}$$

On this basis, the degree of preference for acceptance of positive and negative change β_R is defined according to the individual's personality, and is used to characterize the receiver's tendency to accept the two trends of 'nervousness' and 'non-nervousness' after being informed of the propagator's psychological state. Finally, the expected nervousness during evacuation is obtained by

$$\begin{aligned} \hat{q} &= \beta_R \hat{q}_{\mathrm{D}} + (1 - \beta_R)\hat{q}_{\mathrm{D}} \\ &= \beta_R (1 - (1 - q_S)(1 - q_R)) + (1 - \beta_R) q_S q_R. \end{aligned} \tag{22}$$

The nervous emotion of a single individual during evacuation is affected by all individuals within a certain range at each moment. In the model, only the influence of other pedestrians' psychological states within 5 m of the individual is considered. Individuals whose psychological state can influence the receivers are denoted as the set G. Note that this set does not include the receivers themselves. At this point, the receiver's nervous evacuation emotion changes equation from Eq. (19) to

$$\begin{aligned} \frac{\mathrm{d}q_R(t)}{\mathrm{d}t} &= \sum_{S \in G} \left.\frac{\mathrm{d}q_R(t)}{\mathrm{d}t}\right|_S \\ &= \sum_{S \in G} \gamma_{SR} \left[\beta_R (1 - (1 - q_S)(1 - q_R)) \right. \end{aligned}$$

$$+(1-\beta_R)\,q_S q_R\big]. \tag{23}$$

The psychological state receiver needs to perform one calculation for each psychological sender of nervous evacuation emotion, which is very computationally intensive. The calculation is simplified here by a weighted average of the sender's nervous evacuation emotion under the degree of influence γ, and by replacing each individual's unique evacuation nervous emotion value with the new mean value, which is denoted here as q^*; it is computed by

$$\begin{aligned} q^* &= \sum_{S\in G}\frac{\gamma_{SR}}{\sum\limits_{S\in G}\gamma_{SR}}q_S = \sum_{S\in G}\frac{\varepsilon_S\alpha_{SR}\delta_R}{\sum\limits_{S\in G}\varepsilon_S\alpha_{SR}\delta_R}q_S \\ &= \sum_{S\in G}\frac{\varepsilon_S\alpha_{SR}}{\sum\limits_{S\in G}\varepsilon_S\alpha_{SR}}q_S. \end{aligned} \tag{24}$$

Simplifying Eq. (18) by using q^* as the current nervous emotion during evacuation for each psychological state propagator within the set G, we obtain

$$\begin{aligned} \frac{\mathrm{d}q_R(t)}{\mathrm{d}t} &= \sum_{S\in G}\frac{\mathrm{d}q_R(t)}{\mathrm{d}t}\bigg|_S \\ &= \sum_{S\in G}\gamma_{SR}\big[\beta_R\left(1-(1-q^*)\left(1-q_R\right)\right) \\ &\quad +(1-\beta_R)\,q^*q_R\big]. \end{aligned} \tag{25}$$

Note that currently for any propagator within the set G, the value in parentheses in Eq. (25) is the same. Therefore, the current emotional acceptance strength parameter γ_R of the receiver is defined here, and the method of calculation is as shown in Eq. (26), which ultimately yields the state of the pedestrian's nervous emotion during evacuation over time under the influence of the other pedestrians in the surrounding area, i.e., as shown in Eq. (27). Table 1 systematically shows the meaning of the symbols appearing in Subsection 2.2

$$\gamma_R = \sum_{S\in G}\gamma_{SR}, \tag{26}$$

$$\begin{aligned} \frac{\mathrm{d}q_R(t)}{\mathrm{d}t} &= \gamma_R[\beta_R\left(1-(1-q^*)\left(1-q_R\right)\right) \\ &\quad +(1-\beta_R)q^*q_R]. \end{aligned} \tag{27}$$

Table 1. Parameter interpretation for the model of nervous emotion spreading.

Parameter	Value	Meaning
q	(0,1)	Quantitative value of evacuation nervous emotion
d_{SR}	/	Distance between sender and receiver
ε_S	(0,1)	The propensity of the sender to express psychological states
α_{SR}	$1/d_{SR}$	Channel strength between sender and receiver
δ_R	(0,1)	Receiver's sensitivity to others' psychological states
β_R	(0,1)	Receiver's degree of preference for the reception of nervous emotion
γ_{SR}	$\varepsilon_S\alpha_{SR}\delta_R$	Level of impact between sender and receiver
G	$d_{SR}<5$ m	The set of all senders S that influence the receiver R
γ_R	$\sum\limits_{S\in G}\gamma_{SR}$	The sum of the levels of influence of all S in G
q^*	$\sum\limits_{S\in G}\frac{\varepsilon_S\alpha_{SR}}{\sum\limits_{S\in G}\varepsilon_S\alpha_{SR}}q_S$	Nervous evacuation emotion-weighted mean of all S in G
$\hat{q}_{\mathrm{U}}$	$1-(1-q^*)(1-q_R)$	Receiver's nervous evacuation emotion reaches a maximum
$\hat{q}_{\mathrm{D}}$	q^*q_R	Receiver's nervous evacuation emotion decreases to a minimum

2.3. Attack–escape simulation model

The presence of an attacker in a violent attack has a significant impact on crowd evacuation, with dynamic interactions and even brief confrontations with the attacker during the crowd evacuation process. When people face violent attacks, they often also experience a spreading of nervous emotion, leading to further panic and confusion, which seriously affects evacuation efficiency and the safety of evacuees. Based on the above phenomenon, the attack–escape evacuation simulation model is proposed to simulate the evacuation behavior of crowds under violent attacks.

2.3.1. Attacker simulation model

In a violent attack incident, the attacker's attacking behavior generally manifests itself as a continuous indiscriminate attack. In this paper, we adopt a close-range attack strategy, in which the attacker will directly attack the target person if the distance between the attacker and the target person is close enough. If an evacuee escapes the range of the attacker, the attacker will refrain from chasing and attacking the evacuee and will instead attack someone else nearby. If the distance between the attacker and the nearest person is greater, the attacker will attempt to chase that targeted person with a determined speed to slash. The evacuation behavior ends when all evacuees have escaped from the room in the building. The attacker simulation model is established accordingly.

When the attack event occurs, the attacker k will choose the nearest evacuee i as the target of the attack, and in the characteristic time τ the attacker chases, moving in the direction of the evacuee i with the desired speed by adjusting his actual speed, i.e., this is subject to the effect of the self-driving force. The self-driving force $\boldsymbol{F}_{Dk}$ of the attacker k is given by

$$\boldsymbol{F}_{Dk} = m_k\frac{\boldsymbol{v}_k^0-\boldsymbol{v}_k(t)}{\tau}. \tag{28}$$

During the attack, the attacker needs to constantly chase and cut the evacuees, so the psychological and physical forces generated by the evacuees are negligible for the attacker, who will focus on the forces with the obstacle w. During the attack on the evacuees, the attacker needs to keep a certain distance from the obstacle to avoid possible physical contact, and will also be subjected to a certain amount of elasticity and friction when physical contact with the obstacle occurs. The vector sum f_{ew} of the psychological and physical forces generated by the obstacle w to which the attacker k is subjected is

$$f_{kw} = \sum_w \boldsymbol{F}_{Gkw} + \sum_w \boldsymbol{F}_{Skw}. \tag{29}$$

The set of equations for the evacuation simulation model for attacker k is given by

$$\begin{aligned}
&\boldsymbol{F}_K = m_k \frac{d\boldsymbol{v}_k}{\mathrm{d}t} = \boldsymbol{F}_{Dk} + f_{kw},\\
&\boldsymbol{F}_{Dk} = m_k \frac{\boldsymbol{v}_k^0 - \boldsymbol{v}_k(t)}{\tau},\\
&\boldsymbol{F}_{Gkw} = \mu g(\varepsilon_{kw})\boldsymbol{n}_{kw} + \kappa g(\varepsilon_{kw})(-\boldsymbol{v}_{kw}\cdot\boldsymbol{t}_{kw})\boldsymbol{t}_{kw},\\
&\boldsymbol{F}_{Skw} = A\,\mathrm{e}^{\varepsilon_{kw}/B}\left[\lambda + (1-\lambda)\frac{1+\cos\theta_{kw}}{2}\right]\boldsymbol{n}_{kw},
\end{aligned} \tag{30}$$

where κ and μ are normal quantities representing the strength of the elastic and frictional forces, respectively. A and B are constants measuring the strength and range of action of the psychological force. $\boldsymbol{v}_{kw}$ denotes the velocity of attacker k at the obstacle w. $\boldsymbol{t}_{kw}$ denotes the tangential unit vector between attacker k and obstacle w. $\boldsymbol{n}_{kw}$ is a function that is generated by the physical contact between the individual and the obstacle. Physical forces are generated only when a person is in physical contact with an obstacle, therefore the function $g(\varepsilon_{kw})$ is the greater of ε_{kw} and 0. $\boldsymbol{n}_{kw}$ is a unit vector pointing from attacker k to obstacle w. ε_{kw} denotes the distance between attacker k and obstacle w.

2.3.2. Evacuee simulation model

People tend to choose the nearest exit to escape from fires. However, evacuees in a violent attack often assess risk factors based on the actual attack, avoid the attacker's location and choose an appropriate evacuation route. The shortest evacuation route at this time is not necessarily the safest evacuation route.

The attacker and the evacuee are defined as a circle with a radius of 0.2 m interacting in a room in a building. Calculations yield the conditions for evacuee i to be cut in contact with attacker k shown in Eq. (26)

$$|d_{ki}| \cdot \sin\varphi \le 2r, \tag{31}$$

where r denotes the body radius between the attacker and the evacuee, and the expected time for evacuee i to be chased by attacker k is denoted as T^{C}. When $|d_{ki}|\sin\varphi \le 2r$, the evacuee comes into physical contact with the attacker, at which point the attacker will injure the evacuee, evacuee i will be killed or injured and the evacuation will end, with the evacuee no longer being subject to the attack–escape driving force. The attack–escape drive occurs when evacuees i judge that they will be chased and cut down by an attacker k within time τ. The judgment conditions at this point are analyzed below. In the analysis, using evacuee i as the reference system, the absolute velocity $\boldsymbol{v}_k$ of attacker k is converted to the relative velocity $\boldsymbol{v}_{ki}$ under the reference system of evacuee i. At this point, the attacker k moves relative to i in three states, i.e., chasing i, moving away from i and keeping the relative distance from i unchanged, which corresponds to the three states of $\boldsymbol{v}_{ki}d_{ki}$ greater than 0, less than 0 and equal to 0, respectively.

When $\boldsymbol{v}_{ki}d_{ki} < 0$, evacuee i and attacker k will be far away from each other, the evacuee will not be chased and killed and will choose a suitable evacuation path to escape; when $\boldsymbol{v}_{ki}d_{ki} \ge 0$, the attacker k is chasing the approaching person i or keeping a fixed relative distance between the two, and the expected time to be chased and killed is denoted as T^{C}. When T^{C} is greater than the expected chase threshold τ, it means that the distance between the two is large enough that the attacker k may choose the closer evacuee j as the target of the attack, and therefore there is no need to consider the attack–escape drive force of the attacker k for the evacuee i. When $T^{\mathrm{C}} \le \tau$, the attacker k will chase and kill the evacuee i within the expected time threshold, and then the evacuee i will be subject to the 'chase-and-run' drive. At this point, the possible states of motion are shown in Fig. 2.

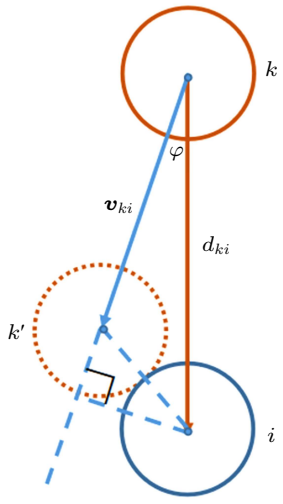


Fig. 2. State of motion between evacuee i and attacker k.

If the evacuee i is in a violent attack event and has not yet been attacked, he or she will observe whether they are the target of the attacker's attack. If they are, the attack–escape driving force will be generated. At this point, the critical state will be $|d_{ki}|\sin\varphi \le 2r$, and the judgment state will be $\boldsymbol{v}_{ki}d_{ki} \ge 0$ and

$T^{\mathrm{C}} \leq \tau$. At this point, the evacuee i will be hacked or killed during physical contact with the attacker. The attack–escape drive force $\boldsymbol{F}_{Ki}$ is determined by the distance and desired speed between attacker k and evacuee i,

$$\boldsymbol{F}_{Ki} = m_i \frac{\left[\boldsymbol{v}_i^0 - \boldsymbol{v}_i(t)\right] \cdot \boldsymbol{v}_{ki} \cdot d_{ki}}{\tau} \cdot d_{ki}. \tag{32}$$

In violent attacks, evacuees are under extreme psychological stress due to the presence of the attacker, and the psychological power of evacuees to maintain a certain distance from other evacuees and obstacles is drastically reduced compared with normal conditions. Therefore, based on the social force model, the model for spread of nervous emotion during evacuation proposed in Subsection 2.2 is introduced to the psychological force of evacuees, which more realistically responds to the evacuation state of pedestrians, and the psychological force $\boldsymbol{F}_{Si}$ of evacuee i during the occurrence of slashing is given by

$$\boldsymbol{F}_{Si} = (1 - q(t))\, \boldsymbol{F}_S. \tag{33}$$

In summary, when evacuee i is attacked in a violent attack event and is the target of the attacker, then the evacuee simulation model equation set is

$$\begin{aligned}
\boldsymbol{F}_i &= m_i \frac{\mathrm{d}\boldsymbol{v}_i}{\mathrm{d}t} = \boldsymbol{F}_{Di} + \boldsymbol{F}_{Gi} + \boldsymbol{F}_{Ki} + \boldsymbol{F}_{Si}, \\
\boldsymbol{F}_{Di} &= m_i \frac{\boldsymbol{v}_i^0 - \boldsymbol{v}_i(t)}{\tau}, \\
\boldsymbol{F}_{Gi} &= \sum\nolimits_j \boldsymbol{F}_{Gij} + \sum\nolimits_w \boldsymbol{F}_{Giw}, \\
\boldsymbol{F}_{Ki} &= m_i \frac{\left[\boldsymbol{v}_i^0 - \boldsymbol{v}_i(t)\right] \cdot \boldsymbol{v}_{ki} \cdot d_{ki}}{\tau} \cdot d_{ki}, \\
\boldsymbol{F}_{Si} &= (1 - q(t))\, \boldsymbol{F}_S, \\
\frac{\mathrm{d}q_R(t)}{\mathrm{d}t} &= \gamma_R \left[\beta_R \left(1 - (1 - q^*)(1 - q_R)\right)\right. \\
&\quad \left. + (1 - \beta_R)\, q^* q_R\right],
\end{aligned} \tag{34}$$

where $\boldsymbol{v}_i^0$ denotes the desired velocity of evacuee i, $\boldsymbol{v}_i(t)$ is the velocity of individual i at moment t, τ is the characteristic time, d_{ki} represents the distance between attacker k and evacuee i and $\boldsymbol{v}_{ki}$ represents the velocity of the attacker towards the evacuee (i.e., the velocity of the assailant minus the velocity of the evacuee).

A flow diagram of whether evacuee i is subject to the attack–escape driving force is shown in Fig. 3.

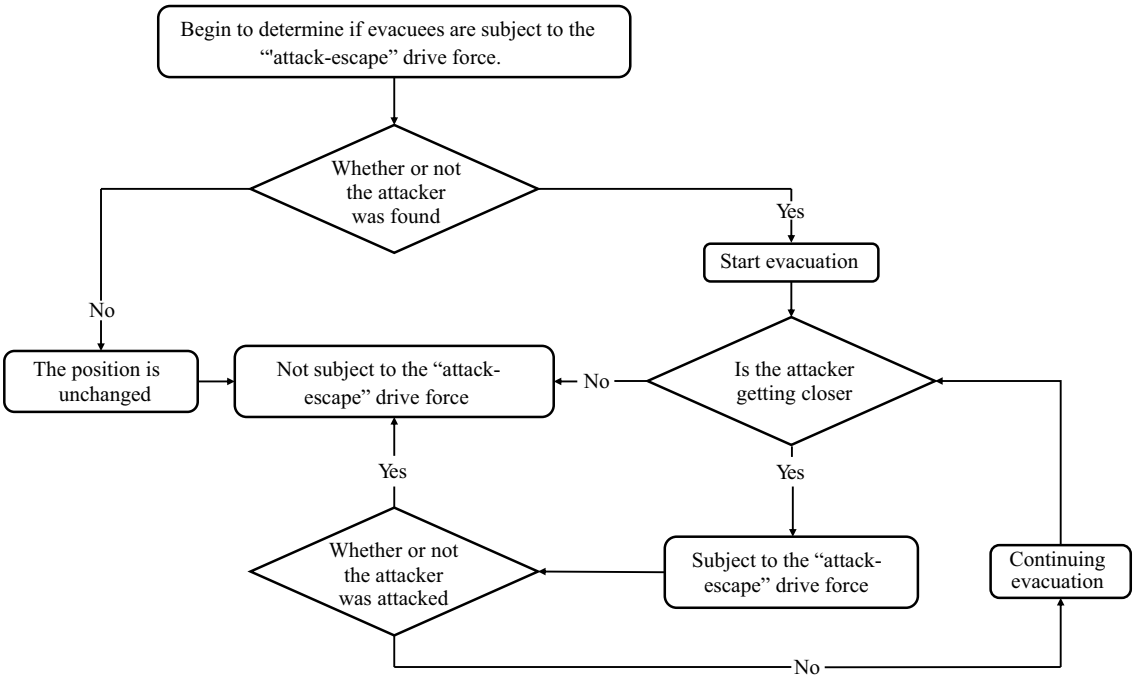


Fig. 3. Flowchart of the conditions for the generation of the attack–escape driving force.

3. Validation and simulation

3.1. Evacuation experiments under attack

We chose experimental locations in two classrooms of a university in China, as shown in Fig. 4. Figure 4(a) shows the standard classroom layout, with each row of tables horizontally spaced 0.6 m apart and each column of tables vertically spaced 1.4 m apart. Figure 4(b) shows an exam classroom layout, with each row of tables horizontally spaced 0.4 m apart and each column of tables vertically spaced 1.2 m. The experiment is divided into four groups. The arrangement of the classroom tables and chairs as well as the attacker's path of attack served as the independent variables in the experiments.

The experiment received ethical approval from the Ethics Committee of the People's Public Security University of China. One hundred students aged 18–20 years (80 male, 20 female) voluntarily participated and were randomly divided

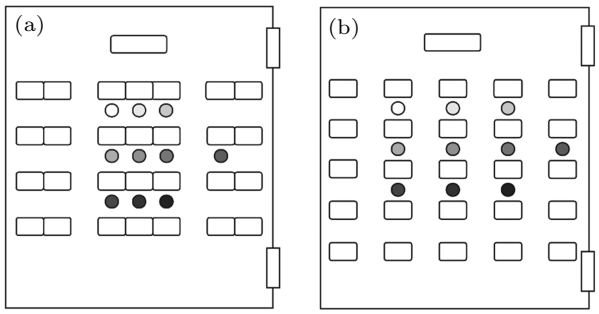


Fig. 4. Classroom floor plan for violent attack evacuation experiment: (a) standard classroom and (b) examination classroom.



Fig. 5. Live views of the violent attack evacuation experiment in the classroom.

into 10 groups of 10. Each participant received $50 after the experiment. Evacuees were familiarized with the experimental site and given a 10-min break after each experiment to mitigate fatigue. The experiment was recorded using two fluorite cameras atop a 2-m high air conditioner, which underwent focal length calibrations before the experiment. Each evacuee wore a distinct colored hat and occupied a designated position. Books were placed on tables to recreate a classroom scenario. The attacker used a 0.5-m model silicone machete to enter through the front or back door and pursued a predetermined route until the last evacuee left, ending the experiment. Experiments 1–4 were conducted sequentially for each group and repeated 40 times in total. A diagram of the experimental procedure is shown in Fig. 5.

3.2. Simulation 1: Validation based on the classroom attack evacuation experiment considering emotion spreading

3.2.1. Simulation setup

Experimental scenarios were reproduced in the simulation, as shown in Fig. 6. The colored circles in the room are evacuees while the black circle at the door represents the attacker. Figure 6(a) shows the simulated standard classroom layout and Fig. 6(b) the simulated examination classroom layout.

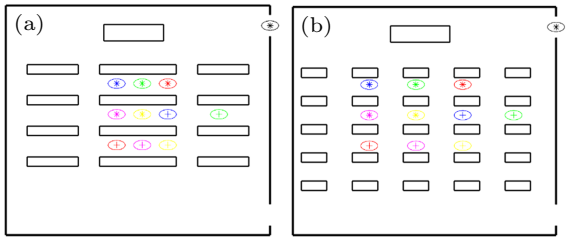


Fig. 6. Schematic of the simulated environment (colored circles in the room are evacuees, the black circle is the attacker): (a) standard classroom and (b) examination classroom.

In the simulation program, 10 evacuees and one attacker are set in the classroom. The attacker adopts two attack strategies: entering from the front door and entering from the back door to attack the two classrooms, respectively, with a total of four simulation programs, as shown in Table 2, and the average value was taken after 30 simulations of each program.

Table 2. Evacuation simulation design for violent attack in a classroom.

Simulation number	Classroom type	Attack route
1	Standard layout	Attacker enters from the front door, chases and slashes along the designated path, and then exits by the back door
2	Standard layout	Attacker enters from the back door, chases and slashes along the designated path, and then exits by the front door
3	Examination layout	Attacker enters from the front door, chases and slashes along the designated path, and then exits by the back door
4	Examination layout	Attacker enters from the back door, chases and slashes along the designated path, and then exits by the front door

3.2.2. Setup of parameters for emotion spreading model

In the nervous emotion model, the values of β_R and γ_{SR} determine the psychological tolerance of the evacuees to a certain extent. Therefore, it is necessary to determine the range of values of β_R and γ_{SR} before the simulation. Considering that the individual parameters are the same when the simulation is performed by the four simulation programs, simulation program 4 is selected for the determination of the nervous emotion parameter during evacuation. As mentioned earlier, the closer β_R and γ_{SR} are to 1, the higher the nervous emotion of the evacuating pedestrian is. Through interviews with subjects who participated in such experiments, we learned that when a violent attack incident occurred in the classroom evacuees were very likely to express their emotions externally under extreme nervous conditions; at the same time, they were very likely to feel the emotional changes of the people around them, which resulted in their evacuation behaviors being in-

fluenced by others. Therefore, in this paper the value of β_R is determined based on a value of 0.9 for ε_S and δ_R.

Figure 7 illustrates how the evacuation time decreases as the value of β_R increases when q is 0.1. When β_R takes a value of 0.9, the evacuation time is reduced by 10.8% compared with when β_R equals 0.1. When the value of β_R reaches 0.7, its effect on the evacuation time begins to decrease, probably because when $\beta_R = 0.7$ the evacuating individual has been extremely susceptible to accepting the nervous emotions of the people around them during evacuation so that he or she reaches a higher level of nervous emotion, thus speeding up the evacuation. When β_R increases further, the effect on the nervous emotion of evacuees is relatively reduced, resulting in a smaller decrease in evacuation time. When $q = 0.9$, the effect of β_R on the evacuation time is very small because the evacuating individual already has very high level of nervous emotion in the initial state and because the effect of β_R on the individual's nervous emotion is small. This results in a slight reduction in the evacuation time, which also illustrates the validity of the mechanism of the spread of nervous emotion during evacuation.

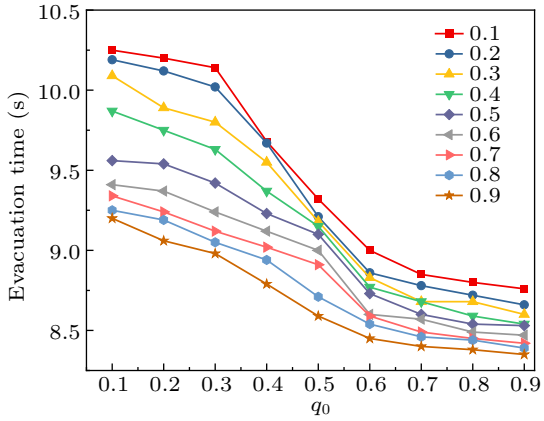


Fig. 7. Changes in evacuation time for different nervous emotion reception preferences and initial levels of nervous emotion.

3.2.3. Simulation results

In this paper, the AEES-SFM is implemented using MATLAB 2021b. The mainframe CPU has a frequency of 2.5 GHz with Windows 11 64-bit being the operating system; 16 GB of RAM is available. The simulation program computes once every 0.02 s with a pedestrian radius of 0.2 m.

3.2.3.1. Evacuation time

The simulation results for reaction time are shown in Fig. 8(a) and those for evacuation time are shown in Fig. 8(b).

As shown in Fig. 8(a), there is a significant difference in reaction times between simulations where the attacker enters through the front door (simulations 1 and 3) and those where the attacker enters through the back door (simulations 2 and 4). When the attacker enters through the front door, evacuees detect the danger immediately and react quickly. Conversely, when the attacker enters through the back door, evacuees can't detect the danger in time and react only when the attacker is close, resulting in a longer reaction time. As shown in Fig. 8(b), evacuation times for simulations 1 and 2 are greater than those for simulations 3 and 4. This may be due to the layout of the examination classroom, where desks are evenly spaced, providing evacuees with more evacuation routes and allowing for flexible evacuation. In the standard layout, desks are grouped, creating a 'barrier' between evacuees and the attacker, making it harder for the attacker to approach directly but also limiting evacuation routes, potentially leading to longer evacuation times due to 'confrontations' with the attacker. There is no positive correlation between reaction time and evacuation time in the simulations. Quick reactions do not always result in faster evacuation. When the attacker enters through the front door, evacuees react quickly but evacuation times are not necessarily shorter than when the attacker enters through the back door. This may be because evacuees start evacuating from a greater distance and choose routes dynamically, potentially leading to confrontations with the attacker and longer evacuation times.

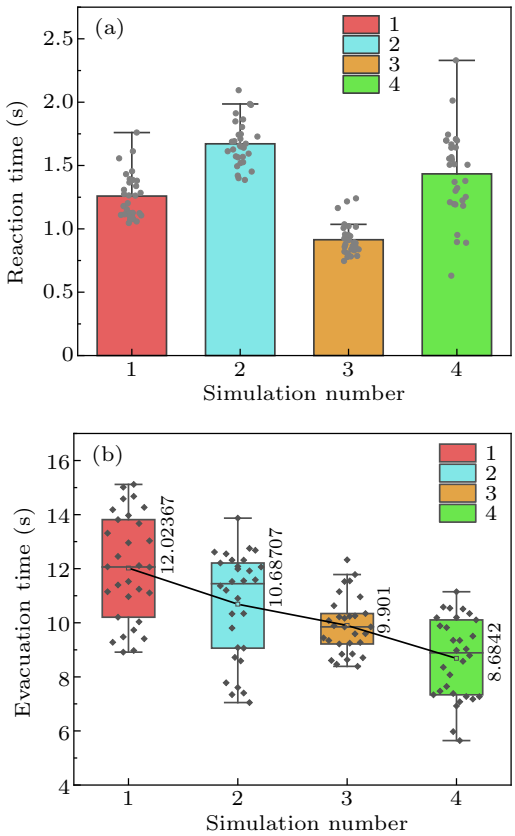


Fig. 8. Simulation results: (a) reaction time simulation results and (b) evacuation time simulation results.

3.2.3.2. Casualties

Figure 9 compares the simulation results for casualties, reaction time and evacuation time. It shows that simulations 1 and 2 had more casualties than simulations 3 and 4. This

may be due to the layout of the exam classroom, where tables and chairs are individually placed allowing evacuees to choose their evacuation direction freely. Compared with the standard layout, individuals are less influenced by others and have more evacuation routes, enabling quick and flexible movement towards exits upon detecting an attacker, thus reducing casualties. An attacker entering through the back door caused more casualties than when entering through the front door, as people were unable to react in time, increasing casualties. This may also explain why evacuation times for simulations 2 and 4 are shorter than those for simulations 1 and 3, respectively. The evacuation time is inversely related to the number of casualties in the same layout. Simulations 1 and 2 had longer reaction times than simulations 3 and 4 due to the decentralized barriers and more routes for attack and evacuation, allowing both attacker and evacuees to move quickly. Reaction time closely relates to the number of casualties and has a significant impact on evacuation success, with shorter reaction times resulting in fewer victims.

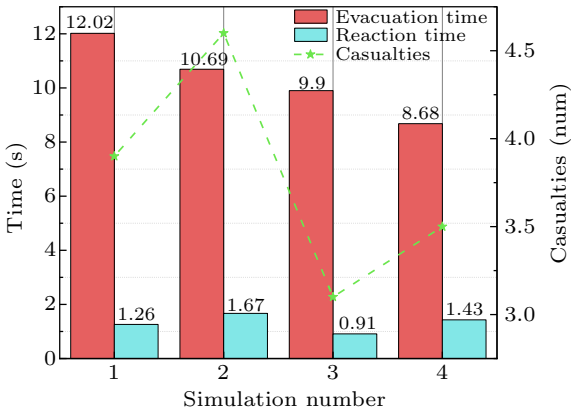


Fig. 9. Comparison of mean values of evacuation time, reaction time and casualty simulation results.

3.2.3.3. Exit choice

This simulation modeled selection of an evacuation exit (Fig. 10). In the standard classroom layout, evacuees tended to choose the door from which the attacker entered as an escape exit, with simulation 1 averaging 3.8 evacuees from the front door and simulation 2 averaging 2.3. In contrast, in the exam classroom layout, evacuees chose the opposite door to the attacker's entry, with simulation 3 averaging 2.5 evacuees from the front door and simulation 4 averaging 4.1. This difference may be related to desk placement. In the standard layout, evacuees were influenced by the side-by-side desk arrangement and chose the door from which the attacker entered. In the exam layout, desks were individually arranged, providing more evacuation path choices and allowing evacuees to choose their evacuation direction at the first opportunity.

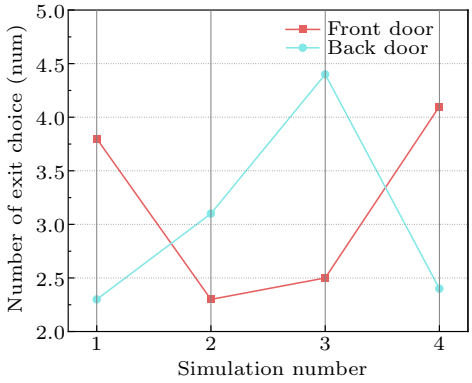


Fig. 10. Variation of the mean value of the simulation results for the number exit choices of evacuees.

3.2.4. Comparison of experimental and simulation results

Figure 11 compares the experimental findings for evacuation time and casualty count with the simulation results, eliminating extreme values. The extreme values in the experimental data were deleted and compared with the simulation results since the simulation was unable to accurately replicate the phenomenon of confrontation between the evacuees and the movement of the attacker in the actual experiment. The modeling and experimental findings for evacuation time and number of casualties, as seen in the figure, are rather similar and within the acceptable range.

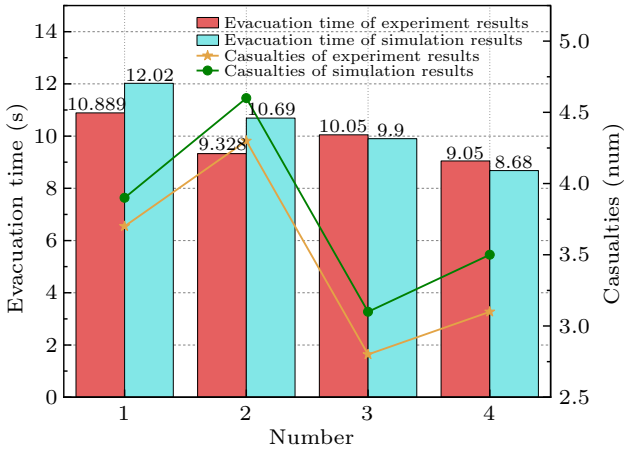


Fig. 11. Comparison of mean values of simulation results for evacuation time, reaction time and casualties.

After the Kolmogorov–Smirnov test, simulation results and experimental results for evacuation time (excluding extreme values) conformed to a normal distribution, while the number of casualties did not conform to a normal distribution. Therefore the *t*-test was used for evacuation time, while the independent samples Mann–Whitney test was used for the number of casualties to determine whether the differences between the simulated and experimental data were significant. The experimental and simulation data were imported into SPSS Statistics 26 for analysis. Table 3 shows the results of the test; the *P*-value is greater than 0.05, which indicates that there is

no significant difference between the experimental data and the simulation results.

Table 3. The *P*-value for the significant difference test between experimental and simulation results.

Category	*P*-value	Whether or not it is significant
Evacuation time	0.090	No
Casualty situation	0.490	No

3.3. Simulation 2: The effect of emotion spread based on simulation results

Once the AEES-SFM has been validated, we went on to simulate the effect of psychological factors on the AEES-SFM in evacuation effectiveness. Snapshots of the simulation process are shown in Fig. 12.

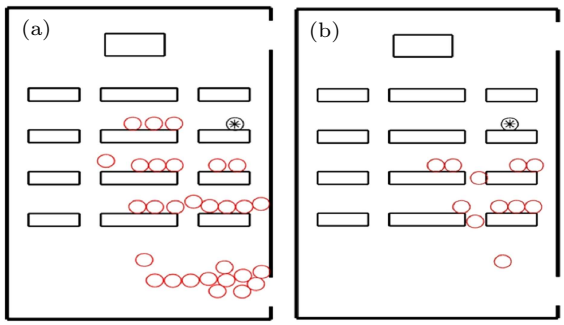


Fig. 12. Snapshots of the simulation: (a) simulation at 4 s and (b) simulation at 16 s.

Several simulations were carried out under two different conditions — evacuation of 10 and 40 people. The simulation results are shown in Fig. 13.

Trends in casualty numbers and evacuation times show similar characteristics as the number of evacuees rises, regardless of psychological influences. However, the influence of psychological factors on evacuation effectiveness varies with different attack modes and classroom layouts. With 10 evacuees, psychological factors slightly reduced evacuation time by up to 30% and casualties by nearly 34%. With 40 evacuees, psychological factors have a greater impact, especially when the attacker enters through the front door in the exam classroom layout. This is because evacuees can start to evacuate promptly and accelerate the process under stronger psychological effects, leading to a greater reduction in evacuation time and casualties than when the attacker enters through the back door. In the exam classroom layout, obstacles (desks and chairs) are more dispersed, providing evacuees with more choices of evacuation route. Nervousness allows them to choose different routes to evade the attacker and accelerate evacuation. Simulation 3 showed the most significant change after considering psychological factors, with substantial decreases in evacuation time and casualties. The results prove the effectiveness of the mechanism of spread of nervous emotion during evacuation.

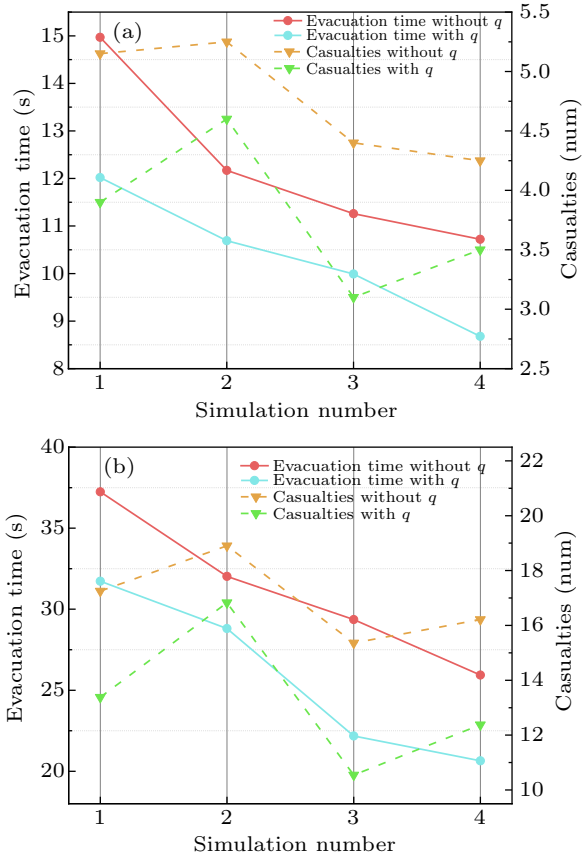


Fig. 13. Effect of nervous emotion on evacuation effectiveness: (a) evacuation results for 10 people and (b) evacuation results for 40 people.

4. Conclusion

In this paper, we propose an attack–escape simulation model, which considers the nerves of the evacuees and improves the social force model in two aspects: the evacuees and the attackers. Two classroom layouts are used as simulation environments to realize the model. The validity of the model was verified by comparing the experimental results with the simulation results by conducting experiments involving violent attack. In addition, the comparison between the simulation results for 10 and 40 people shows that the influence of emotions on the evacuation results becomes larger as the number of people increases, proving the validity of the model of emotion spreading.

Our results show that (1) there is no association between the length of time it takes to evacuate and the number of casualties, suggesting that the reaction time of those being evacuated has a significant influence on whether they can do so successfully; (2) dispersed placement of desks and chairs in the classroom is more convenient for the evacuation of personnel and effectively reduces the number of casualties; (3) there is a relationship between the attacker's attack route and the number of casualties: higher casualties were inflicted by the attacker coming through the classroom's back entrance, indicating that the attacker's original location had a greater bearing on the number of injuries; (4) with the same attack strategy

and different classroom layouts, the evacuees reflected opposite exit selection tendencies, which were mainly related to the placement of desks and chairs in the classroom.

There are some limitations to our study. (1) Due to the limitations of the experimental conditions, the subjects in the experiment were all college students in good physical condition, and primary and secondary school students were not involved. Compared with primary and secondary school students, college students are more versatile in thinking and act more quickly. (2) The simulation and experiments are localized scenes that do not involve evacuation behavior outside the classroom and there is only one attacker, which may be different from reality. In the future, we will use virtual reality to conduct more realistic global evacuation experiments among subjects of different age groups and use the obtained experimental data to analyze the characteristics of individual evacuation behaviors as well as to adjust the parameters in the simulation model to further study the law of students' evacuation behaviors in the context of violent attacks, and to provide assistance for the development of emergency response plans for violent attacks on campuses and students' evacuation drills.

Acknowledgement

Project supported by the National Natural Science Foundation of China (Grant No. 72274208).

References

[1] Schwarz E D and Kowalski J M 1991 *Journal of the American Academy of Child & Adolescent Psychiatry* **30** 936
[2] Livingston M D, Rossheim M E and Hall K S 2019 *Journal of Adolescent Health* **64** 797
[3] Hilal S M, Densley J A, Li S D and Ma Y 2014 *Homicide Studies* **18** 83
[4] Wang J, Ni S J, Shen S F and Li S Y 2019 *Physica A* **523** 1
[5] Lu P, Zhang Z, Li M D, Chen D H and Yang H 2020 *Knowledge-Based Systems* **205** 106291
[6] Jonson C L, Moon M M and Hendry J A 2020 *Journal of School Violence* **19** 154
[7] van der Wal C N, Robinson M A, de Bruin W B and Gwynne S 2021 *Safety Science* **136** 105121
[8] Liu Q 2020 *International Journal of Disaster Risk Reduction* **46** 101605
[9] Deng K F, Li M, Hu X M and Chen T 2024 *Chin. Phys. B* **33** 028901
[10] Cai Z Y, Zhou R, Cui Y K and Jiang J C 2023 *Chin. Phys. B* **32** 020507
[11] Yang X X, Jiang H L, Kang Y L, Yang Y, Li Y X and Yu C 2022 *Chin. Phys. B* **31** 078901
[12] Liu Q 2018 *Physica A* **502** 315
[13] Arteaga C and Jee W P 2020 *Safety Science* **127** 104692
[14] Liu J M, Zhang H, Ding N and Li Y T 2024 *Physica A* **633** 129403
[15] Shang H Y, Feng P F Zhang J and Chu H R 2023 *Transportmetrica A: Transport Science* **19** 1995529
[16] Zheng L J, Peng X L, Wang L L and Sun D H 2019 *Physica A* **522** 167
[17] Helbing D and Peter M 1995 *Phys. Rev. E* **51** 4282
[18] Gao Y, Chen T, Peter B L and Zhang H 2017 *Fire Technology* **53** 331
[19] Ding N, Zhu Y, Liu X Y, Dong D P and Wang Y 2024 *Applied Mathematics and Computation* **466** 128448
[20] Yang L Y and Ding N 2023 *Safety Science* **166** 106243
[21] Bosse T, Duell R, Memon Z A, Treur J and Van Der Wal C N 2009 In *Principles of Practice in Multi-Agent Systems:* 12*th International Conference*, December 14–16, Nagoya, Japan, p. 48
[22] Bosse T, Duell R, Memon Z A, Treur J and Van Der Wal C N 2015 *Cognitive Computation* **7** 111